Journal of Environmental Management 300 (2021) 113823

Contents lists available at ScienceDirect

Journal of Environmental Management

journal homepage: www.elsevier.com/locate/jenvman

Predicting forested wetland soil carbon using quantitative color sensor measurements in the region of northern Virginia, USA

Stephanie A. Schmidt, Changwoo Ahn *

Department of Environmental Science and Policy, George Mason University, 4400 University Drive, MS5F2, Fairfax, VA, 22030, USA

ARTICLE INFO

Keywords:
Soil color
Forested wetlands
Soil carbon
Nix Pro color sensor
Coastal Plain
Piedmont

ABSTRACT

Forested wetland soils within the Piedmont and Coastal Plain physiographic provinces of Northern Virginia (NOVA) were investigated to determine the utility of a handheld colorimeter, the Nix Pro Color Sensor ("Nix"), for predicting carbon contents (*TC*) and stocks (*TC stocks*) from on-site color measurements. Both the color variables recorded with each Nix scan ("Nix color variables"; n = 15) and carbon contents significantly differed between sites, with redder soils (higher *a* and *h*) at Piedmont sites, and higher TC at sites with darker soils (lower values of *L*, or lightness; $p < 0.05$). Nix–carbon correlation analysis revealed strong relationships between *L* (lightness), *X* (a virtual spectral variable), *R* (additive red), and K_K (black) and log-transformed TC (Ln[TC]; $|r| = 0.70$; $p < 0.01$ for all). Simple linear regressions were conducted to identify how well these four final Nix variables could predict soil carbon. Using all color measurements, about 50% of Ln(TC) variability could be explained by *L*, *X*, *R*, or K_K ($p < 0.01$), yet with higher predictive power obtained for Coastal Plain soils ($0.55 < R^2 < 0.65$; $p < 0.01$). Regression model strength was maximized between Ln(TC) and the four final Nix variables using simple linear regressions when color measurements observed at a specific depth were first averaged ($0.66 < R^2 < 0.70$; $p < 0.01$). While further study is warranted to investigate Nix applicability within various soil settings, these results demonstrate potential for the Nix and its soil color measurements to assist with rapid field-based assessments of soil carbon in forested wetlands.

1. Introduction

Estimated to hold over 2300 Gt C in its top 3 m, soil is one of the largest carbon reservoirs on Earth (Jobbágy and Jackson, 2000; Köchy et al., 2015; Schlesinger, 1990). Efforts to minimize soil carbon losses and augment soil carbon sequestration have assumed a prominent role in natural climate solutions, given the key role that soil organic carbon (SOC) dynamics play in regulating atmospheric greenhouse gases (GHGs) (Bossio et al., 2020; Guo and Gifford, 2002; Sahoo et al., 2019). Wetlands have received particular attention for their carbon storage potential due to high rates primary productivity paired with anaerobic biogeochemical settings that slow decomposition of organic matter (Mitsch and Gosselink, 2015; Villa and Mitsch, 2015). Some wetland types, such as subarctic peatlands with thawing permafrost, tend to act as carbon sources rather than sinks (Johansson et al., 2006); conversely, wetlands with mineral soils, including forested palustrine wetlands, can serve as promising carbon sinks due to a seasonal or intermittent reduction of the soil environment that slows decomposition of recalcitrant soil organic matter (SOM), encourages high productivity, and minimizes methane emission potential (Bernal and Mitsch, 2013; Bridgham et al., 2006; Chimner and Ewel, 2005; Villa and Bernal, 2018; Villa and Mitsch, 2015; Whiting and Chanton, 2001). In areas with natural forested wetland cover, their conservation and restoration have thus become attractive strategies to counter GHG emissions through augmented soil carbon sequestration (Bae and Ryu, 2015; Pulighe et al., 2016; Säynäjoki et al., 2018; Virginia Department of Environmental Quality, 2019; Xue et al., 2019).

Measuring SOC within the top 30 cm of forested wetland soils where carbon concentrations and fluxes are highest can be useful for drafting climate adaptation strategies, for which preliminary assessments and sustained monitoring of carbon storage potentials and fluxes are essential (Lees et al., 2018; Nahlik and Fennessy, 2016; Yu et al., 2012). Furthermore, estimates of SOC can aid wetland ecosystem health and development assessments through the connection between SOC and root development, water retention and infiltration rates, cation exchange and buffering capacity, and reduction-oxidation reactions with nitrate-nitrite and iron/manganese (Ahn and Jones, 2013; Bishel-Machung et al., 1996). Therefore, measuring SOC over time can provide

* Corresponding author.
E-mail address: cahn@gmu.edu (C. Ahn).

https://doi.org/10.1016/j.jenvman.2021.113823
Received 5 May 2021; Received in revised form 11 September 2021; Accepted 22 September 2021

critical information to watershed planners, managers, and scientists. Because current estimates of SOC commonly rely on laboratory analyses that are unavailable at the time of field observations and require great expense, labor, and time (Meersmans et al., 2009; Post et al., 2001; Rawlins et al., 2008; Roper et al., 2019), various methodology-focused studies have sought to link SOC to more rapid and/or accessible field- or laboratory-based measurements.

Soil color has emerged as a strong predictor of SOC and soil total carbon (TC) contents (Pretorius et al., 2017; Stiglitz et al., 2017; Wills et al., 2007), with researchers first linking soil darkness to SOM as early as the 1920s (Brown and O'Neal, 1923). Using A.H. Munsell's Munsell Soil Color Chart (MSCC) that standardizes perceived colors via observations of *hue*, *value*, and *chroma* (Munsell, 1905), color variables—most notably value and chroma—have been shown to be strong predictors of SOC (Konen et al., 2003; Pretorius et al., 2017; Wills et al., 2007). The MSCC is nonetheless imperfect for rapid field-based determinations and SOC predictions, as it is dependent on factors that introduce error into measured colors: aging of the MSCC color chips, soil texture and moisture, lighting conditions, subjective color judgments, and training that is required to increase user familiarity (Elliot, 2015; Neitz et al., 2002; Sánchez-Marañón et al., 2011; Schmidt and Ahn, 2019; Torrent and Barrón, 1993). Additionally, the MSCC relies on semiquantitative data and requires transformations for statistical analysis (Kirillova et al., 2015; Viscarra Rossel et al., 2009). Other soil color methodologies have been utilized to identify and quantify soil colors, with various devices like mobile phone cameras, handheld spectrophotometers, and handheld colorimeters investigated as rapid field-based methods to complement and/or substitute for the MSCC in field monitoring. Cameras can capture an entire soil profile for color determination but require color correction cards, standardized photography conditions, and specific processing algorithms to accurately and reproducibly determine color (Aitkenhead et al., 2015; Han et al., 2016). Handheld spectrophotometers and colorimeters can greatly aid in rapidly and objectively identifying soil colors, but can cost over $1000 compared to the more accessible $250 of the MSCC; furthermore, both suffer from error introduced from light scattering through heterogeneity in soil texture and surface evenness that renders them more suitable for laboratory-based methodologies (Fan et al., 2017; Gómez-Robledo et al., 2013; Moritsuka et al., 2014; Stiglitz et al., 2016; Schmidt and Ahn, 2021).

The Nix Pro Color Sensor (*"Nix"*; www.nixsensor.com/nix-pro/) is an app-based color measurement device that can be complementary to the MSCC with a similar price ($349) (Schmidt and Ahn, 2021). Through its continuous numerical and objective measurements of soil color using 15 variables from 5 color spaces including the Commission on Illumination (CIE) $L^*a^*b^*$ (CIE–Lab), it represents an opportunity to predict SOC from field-based soil color measurements (see Schmidt and Ahn [2021] for further information about color spaces and color variables). While strong relationships between the Nix and SOC have been established—with coefficient of determination (R^2) strengths up to 0.98 (Mukhopadhyay et al., 2020; Mikhailova et al., 2017; Stiglitz et al., 2018)—all investigations have focused on upland soils in specific geographic settings, and have relied on lab-based methods using dried and homogenized soils for color determinations. Field assessments that target different physiographic, hydrologic, and ecological settings are necessary to more fully assess the Nix's capability to assess soil carbon from on-site color determinations.

The goal of this study was thus to explore the potential use of a quantitative color sensor, the Nix, to predict carbon contents and stocks in the top layer of forested wetland soils. By using total carbon (TC) as a proxy for SOC in a non-calcareous soilscape, research objectives were to (1) collect, assess, and compare (a) field-based soil color data using the Nix color sensor and (b) soil carbon contents and stocks across different sites and physiographic provinces in NOVA; (2) assess relationships between all color variables collected by the Nix and soil carbon contents and stocks via correlation analysis; and (3) identify predictive power of single and multiple linear regression models relying on Nix color variables to predict soil carbon.

2. Material and methods

2.1. Site description

Field research was carried out in 2020 at four forested wetlands in Northern Virginia: Algonkian Regional Park (ARP), Banshee Reeks Nature Preserve (BR), Julie J. Metz Wetlands Bank (JJM), and Elizabeth Hartwell–Mason Neck National Wildlife Refuge (MN) (Fig. 1). Sites were selected to be balanced across the Piedmont (ARP, BR) and Coastal Plain (JJM, MN) physiographic provinces. Each site was sampled at 5 randomly selected plots spaced at least 200 m apart (Chi et al., 2018). Table 1 describes the characteristics of the four sites, including geomorphology, dominant soils, and vegetation communities.

In the Piedmont, ARP (39°3′28″ N, 77°21′51″ W) includes riparian forests and freshwater forested and emergent wetlands influenced by overland flow from the Potomac River, groundwater connection with nearby wetlands, and precipitation. Mapped soil series include Rowland silt loams and Lindside silt loams; while neither is hydric, ARP was observed to be capable of supporting wetland vegetation before sampling began (USDA–NRCS Soil Survey Staff, 2020). BR (39°1′31″ N, 77°35′30″ W) includes occasionally to frequently saturated forested areas mapped as the hydric Albano silt loam plus the nonhydric Codorus and Manassas silt loams (USDA–NRCS Soil Survey Staff, 2020). Floodplains and riparian zones are influenced by subsurface flow from Goose Creek, precipitation, and surface runoff from tributaries.

In the Coastal Plain, JJM (38°36′23″ N, 77°16′38″ W) lies adjacent to Neabsco Creek, a tributary of the Potomac River, and has sustained wetland hydrology since its construction as a mitigation wetland in 1994 (Environmental Laboratory, 1987). The wetland contains occasionally, frequently, and permanently flooded soils mapped as the hydric Feathertone mucky silty loam and Hatboro-Codorus Complex, which are influenced by groundwater recharge, precipitation, and stream surface flow (USDA–NRCS Soil Survey Staff, 2020). MN (38°38′38″ N, 77°09′57″ W) includes a hardwood forest and forested wetland with rolling microtopography consisting of high points (hummocks) and low points (hollows). The occasionally to frequently saturated hollows are mainly influenced by precipitation and are mapped as the hydric Gunston silt loams; the rarely saturated hummocks are mapped as the nonhydric Matapeake silt loams and Mattapex loams (Ahn et al., 2009; USDA–NRCS Soil Survey Staff, 2020).

2.2. Field methods

Soils were sampled in spring (March–April), summer (June–July), and fall (August–September) of 2018 and 2019 to capture seasonal fluctuations in color over two growing seasons. Average temperatures were 56.3° F (7° F to 95° F) in 2018 and 57.2° F (−2° F to 100° F) in 2019; total precipitation was 169.5 cm in 2018 and 103.7 cm in 2019, with 2018 being the wettest year of the decade by over 50 cm (Menne et al., 2012). At each plot (n = 16), a 10-cm (4″) diameter auger (AMS) was used for soil profiling; while augering cannot provide an in-tact and undisturbed core from sampling, it provides an adequate sample size for identifying present soil colors in a relatively short time period without large plot disturbance, allowing it to be scaled to both professional and nonprofessional soil investigations (O'Donnell et al., 2011).

After removing surface debris, soil was augered down to 60 cm and laid on a white sheet to reflect in-situ soil horizonation. For each 10-cm depth interval (0–10 cm, 10–20 cm, and 20–30 cm), peds were split and identified interior colors were scanned with the Nix after it was connected to an Android smartphone running the Nix Pro Color Sensor app, which automatically recorded and stored scanned colors alongside timestamps and typed descriptors. Each scan is composed of 15 *Nix color variables* (grouped by color spaces, with names related to their respective

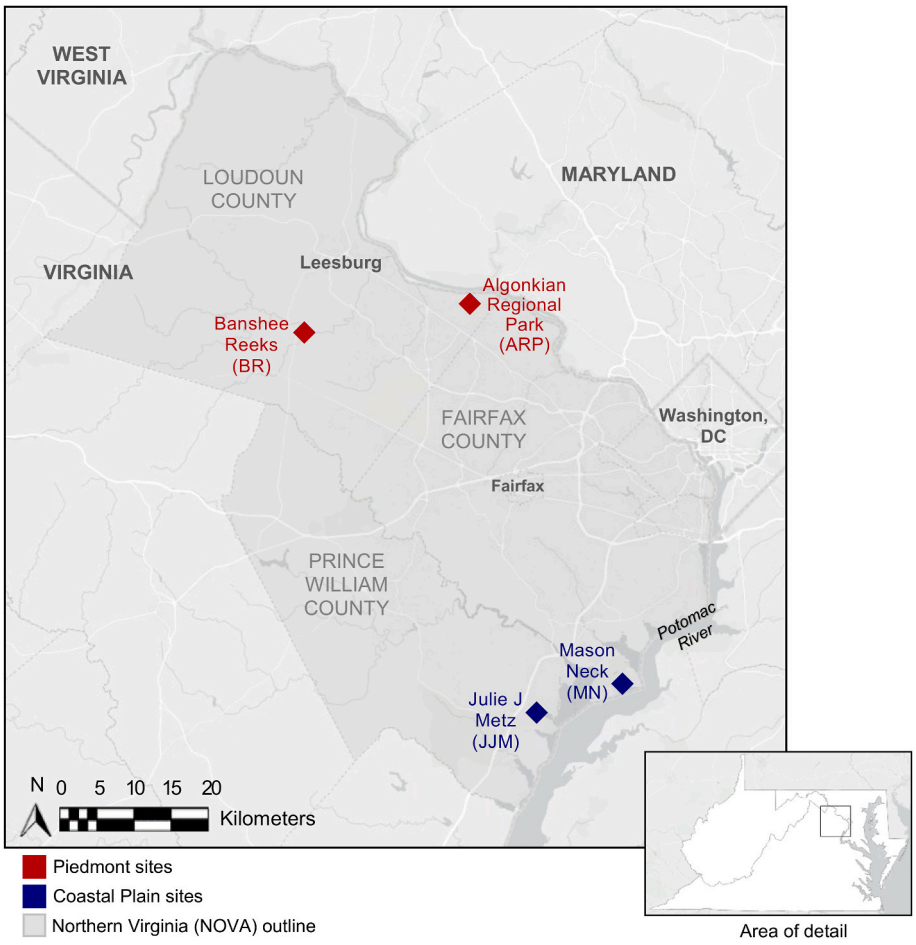

Fig. 1. Locations of the four forested wetland study sites in northern Virginia, USA.

Table 1
Site descriptions including landscape, vegetative, and soil characteristics.

	Algonkian Regional Park (ARP)	Banshee Reeks (BR)	Julie J. Metz Neabsco Creek (JJM)	Mason Neck (MN)
Physiographic Province	Piedmont	Piedmont	Coastal Plain	Coastal Plain
Geologic Age	Upper Triassic	Upper Triassic	Quaternary	Quaternary
Primary Texture Classes [a]	Silt loam	Silt loam (cobbly/gravelly)	Silt loam, sandy loam (mucky, cobbly/ gravelly)	Silt loam, loam
Major Vegetation community	Black walnut and oak forested floodplains; freshwater forested wetlands; freshwater emergent wetland	Hardwood forests, riparian zones, forested wetlands, & Mountain-Piedmont basic seepage swamp	Forested, scrub, and emergent wetlands	Hardwood oak- hickory forests, palustrine forested wetland

[a] USDA-NRSC Soil SurveyStaff (2020).

variables): *L*, *a*, *b* (CIE–Lab), *C*, *h* (CIE–LCh), *X*, *Y*, *Z* (CIE–XYZ), *R*, *G*, *B* (RGB), and C_K, M_K, Y_K, and K_K (CMYK) (Schmidt and Ahn, 2021). After initial scans, peds were iteratively halved along structural voids to form smaller peds; for each 10-cm depth interval, newly identified interior colors were also scanned using the Nix. This process was repeated until a ped diameter of 3–5 cm was reached or until peds were unable to maintain an even intact surface for Nix color recording. Before using the Nix, soils were wetted if dry, and surfaces were smoothed without mixing colors to create an even surface. Independent of ped boundaries, perceptibly identical colors within a given soil horizon were not repeatedly scanned. Colors were not measured when they could not fit within the Nix aperture (i.e., features less than 1 cm in diameter).

At three subplots per plot, soil samples were obtained for bulk density (D_b) and carbon analyses using a probe handcrafted from a PVC pipe with saw-tooth edges and notches at 10, 20, and 30 cm (modified from Caldwell et al., [2005] and Giannopoulos et al., [2019]). Undisturbed 30-cm cores were sampled and separated into three equally sized 10-cm depth intervals (0–10 cm, 10–20 cm, and 20–30 cm). Because one plot at both JJM and BR included large rocks below 20 cm (diameters > 5–10 cm), 20–30 cm samples were not collected at 6 subplots, totaling 138 soil samples collected for both D_b and carbon analysis (i.e., 4 sites • 4 plots • 3 subplots • 3 depth intervals = 144 minus 6).

2.3. Lab analysis

Wet masses were obtained for 10-cm-length soil core samples within 4 h of collection using a Sartoruis Miras 2 scale with 5 g readability. Samples were placed into a drying oven between 85 °C and 105 °C for at

least 72 h until a constant dry mass was achieved; D_b (g•cm^{-3}) was subsequently calculated as the ratio between soil dry mass and the soil probe core volume.

Dried soil cores were crushed using a mortar and pestle then passed through a 2-mm sieve three times. Dry-weight percentages of total carbon (*TC*) were obtained from 5 to 10 mg samples using a PerkinElmer 2400 Series II CHNS/O Analyzer (PerkinElmer Corporation, Norwalk, CT, USA). Total carbon stocks (*TC stocks*, kgC•m^{-2}) were calculated at each depth interval by multiplying TC, D_b, and interval length (10 cm) and converting to proper units: *TC stocks* = D_b [g•cm^{-3}] • 10 cm • 10^4 cm^2/m^2 • (*TC* [%]/100) [g C/100 g] • 1/10^3 kg/g C; i.e., *TC stocks* (kgC•m^{-2}) = D_b • *TC*. TC and TC stocks are herein referred to as *carbon variables*. TC (stocks) for the region's Piedmont and Coastal Plain are virtually equivalent to SOC (stocks) given the non-calcareous nature of the studied soilscape (Konen et al., 2003).

2.4. Data Analysis

Using Microsoft (MS) Excel (Version, 2012, 2021), carbon contents and bulk densities were averaged across subplots to yield plot-specific TC (%) and TC stock calculations for 0–10 cm, 10–20 cm, and 20–30 cm depth intervals. Soil color measurements were subsequently matched with plot averages for carbon contents and stocks. Data were scanned and screened to remove (1) outliers, defined as colors that fell outside 2 standard deviations of the mean for a given TC percentage, or coordinate pairs with simple linear regression residuals exceeding 3% in TC for Nix color variable *L*; (2) non-matrix redoximorphic features (gley colors, depletions, and concentrations); and (3) duplicates (e.g., identical color scans taken from same color at a specific plot and depth interval), leaving a sample size of 134. These samples are referred to as the *aggregate dataset* (n = 134), comprised of all recorded colors and respective soil carbon contents and stocks for all study plots and depth intervals (e.g., one sample would include a color observed at JJM plot 2 from 10 to 20 cm with its respective carbon contents and stocks).

After verifying assumptions of normality and homogeneity of variances on color and carbon variables, ANOVA, correlation, and regression analyses were conducted. Correlation analysis was conducted between Nix color variables and carbon contents and stocks plus three transformations of carbon contents and stocks (natural log [Ln(x)], square root [$\sqrt{x}$], and inverse [x^{-1}]), which were included to potentially strengthen correlations and regressions (Becker et al., 2019; Pek et al., 2019). Pearson correlations between measured Nix color variables and measured and transformed carbon variables were evaluated to yield finally-chosen *(final)* Nix color variables and one finally-chosen *(final)* carbon variable with priority placed on measured variables, but ultimately based on strength of correlations; $|r| \geq 0.70$ was used to indicate strong correlations (Akoglu, 2018; Dancey and Reidy, 2007; Mukaka, 2012). For Nix color variables of the same color space with similar correlation coefficients ($|\Delta r| \leq 0.02$), a maximum of one variable was selected on the basis of user familiarity and innate relation to colors common in soil (e.g., from RGB, *R* [red] is more perceptually relevant for describing soil color than *G* [green]).

Final Nix color variables were used in four subsequent regression analyses. First, using the aggregate dataset, linear regression models were conducted on soil carbon and each final Nix color variable; scatterplots were also visually assessed to identify nonrandom patterns in residuals. To identify if relationships depended on physiographic province, regressions were also conducted using data separated by levels of each factor (i.e., physiographic province [factor] separated by Piedmont and Coastal Plain [factor levels]). Third, to remove noise in the regression models conducted on the aggregate dataset—in which each plot and depth interval had more than one corresponding color observed— linear regression models were conducted on soil carbon using Nix color variables that were averaged at each carbon percentage level (i.e., averaged by each plot and depth interval). Finally, using IBM SPSS software (Version 26, 2019), a backward stepwise multiple linear regression (MLR) model was also conducted with all Nix color variables as inputs to assess the added value of employing multiple Nix color variables in soil carbon predictions.

3. Results

3.1. Soil color and carbon by site

Table 2 displays all quantitative Nix color variables as well as TC and TC stocks for study sites. Colors showed high variability for several Nix color variables, specifically Lab L, or lightness (13.2–60.5) and CMYK K_K, or black (0.06–0.76). Variability depended on site for certain variables, where LCh *C* (i.e., chroma) was the only variable that did not significantly differ between sites (Table 2; $p > 0.10$). Piedmont soils (ARP, BR) showed higher values of Lab *a* and lower values of LCh *h*—both indicative of redder hues—than Coastal Plain soils (JJM, MN; $p < 0.05$). In contrast, CMYK M_K, magenta, and RGB *R*, red, did not significantly differ due to the combination of lightness and hue in these subtractive (CMYK) and additive (RGB) color spaces. With respect to soil lightness (corresponding to MSCC value), BR and JJM soils were significantly darker than MN soils, with lower Lab L (lightness) and higher CMYK K_K (black) ($p < 0.01$); coinciding with these differences, JJM soils had lower values of RGB *R* (additive red) and *B* (additive blue) compared to ARP and MN ($p < 0.05$), where lower values of RGB *R*, *G*, and *B* in tandem relate to darker soils. While MN contained lighter soils than JJM and BR as seen through differences in *L*, *R*, *G*, and *B* ($p < 0.05$),

Table 2
Nix color variables (n = 15) from five color spaces and carbon contents and stocks measured at each forested wetland site (mean ± standard error).

	Algonkian Regional Park (ARP)	Banshee Reeks (BR)	Julie J. Metz Neabsco Creek (JJM)	Mason Neck (MN)
Nix Color Variables				
Lab				
L **	37.9 ± 3.0 ^{ab}	34.4 ± 5.1^{b}	27.3 ± 4.0^{b}	42.2 ± 11.3^{a}
a **	9.9 ± 1.0^{a}	8.4 ± 3.1^{a}	5.6 ± 0.6^{b}	6.6 ± 2.3^{b}
b *	15.7 ± 1.2^{a}	16.4 ± 3.4^{a}	13.9 ± 1.5^{a}	18.1 ± 6.7^{a}
LCh				
C	18.6 ± 1.5 c	18.5 ± 4.3 c	14.9 ± 1.6 c	19.3 ± 7.0 c
h **	57.6 ± 1.3^{c}	63.6 ± 5.3^{b}	68 ± 1.1^{a}	69.3 ± 4.9^{a}
XYZ				
X **	10.4 ± 1.8^{b}	9.2 ± 2.9^{b}	5.6 ± 1.4^{b}	14.8 ± 7.4^{a}
Y **	9.5 ± 1.6^{b}	8.5 ± 2.5^{b}	5.3 ± 1.4^{b}	14.3 ± 7.2^{a}
Z **	4.5 ± 0.9^{b}	3.7 ± 1.0^{b}	2.4 ± 0.7^{b}	6.4 ± 3.0^{a}
RGB				
R **	108.0 ± 8.3 ^{ab}	100.1 ± 16.1 ^{bc}	78.3 ± 10.3^{c}	118.6 ± 34.8^{a}
G **	80.3 ± 7.1^{b}	75.8 ± 11.0^{b}	61.2 ± 8.7^{b}	96.2 ± 28.6^{a}
B **	61.7 ± 6.8 ^{ab}	55.4 ± 7.8 ^{bc}	43.7 ± 7.3^{c}	70.4 ± 19.9^{a}
CMYK				
C_K **	0.46 ± 0.02^{b}	0.48 ± 0.05 ^{ab}	0.53 ± 0.02^{a}	0.45 ± 0.08^{b}
M_K **	0.60 ± 0.02^{a}	0.60 ± 0.03^{a}	0.61 ± 0.02^{a}	0.53 ± 0.07^{b}
Y_K **	0.72 ± 0.02^{b}	0.75 ± 0.02^{a}	0.77 ± 0.02^{a}	0.71 ± 0.04^{b}
K_K **	0.36 ± 0.05 ^{bc}	0.40 ± 0.09 ^{ab}	0.52 ± 0.07^{a}	0.29 ± 0.19^{c}
Soil Carbon				
TC (%)**	1.19 ± 0.35^{b}	2.31 ± 1.01^{a}	2.87 ± 0.35^{a}	1.24 ± 1.14^{b}
TC Stocks (kg•m^{-2}) **	1.5 ± 0.3^{c}	3.1 ± 1.1^{b}	4.3 ± 1.0^{a}	1.5 ± 1.1^{c}

*p < 0.05.
**p < 0.01.

MN also included the largest range for almost all Nix color variables—specifically Lab L (lightness), LCh *C* (chroma) and *h* (hue), RGB *R* (additive red), *G* (additive green), and *B* (additive blue), and CMYK C_K (cyan) and K_K (black) (Table 2).

Table 2 also displays carbon characteristics at each site, represented as TC (%) and TC stocks (kg•m^{-2}) where the latter is reported only for the top 10 cm that was responsible for the majority (>50%) of soil carbon from 0 to 30 cm. Average TC and TC stocks ranged from 0.34% to 4.11% and from 0.40 kg m^{-2} to 5.7 kg m^{-2}, respectively, with values that were comparable to other studies on Mid-Atlantic Piedmont and Coastal Plain forested wetlands in or near NOVA. However, several plots included TC and TC stocks not indicative of wetland development, e.g., TC < 2–3% (Giese and Flannagan, 2006; Giese et al., 2000); in particular, ARP plots were consistently low in TC (0.9%–2.0%; $p > 0.05$) and significantly lower in TC stocks (1.2–2.0 kg m^{-2}; $p < 0.05$) compared to other sites. Conversely, JJM plots were consistently high in TC (2.6%–3.3%; $p > 0.05$) with higher TC stocks than other sites (3.6–5.7 kg m^{-2}; $p < 0.05$). While BR and MN had higher variability in TC (1.3%–4.1% and 0.3%–4.1%, respectively), both included the study's highest reported carbon contents (>4.0%), where MN's carbon content variability matches its high variability in Nix color variables (Table 2).

Significant differences in TC between sites, with higher TC at BR and JJM than ARP and MN ($p < 0.01$), mirrored several trends in soil color variable differences between sites—for example, BR and JJM soils had lower values of Lab L (34.4 ± 5.1; 27.3 ± 4.0) than MN (42.2 ± 11.3; $p < 0.05$) and ARP (37.9 ± 3.0; $p < 0.10$); and higher values of CMYK K_K (0.40 ± 0.09; 0.52 ± 0.07) than MN (0.29 ± 0.19; $p < 0.05$) and ARP (0.36 ± 0.05; $p < 0.10$), respectively, indicating a link between color lightness (*L*) or darkness (K_K) and soil carbon.

3.2. Correlations

Table 3 shows the correlation results between Nix color variables and carbon contents and stocks; in addition to TC and TC stocks, natural log transformations (but neither square root nor inverse transformations) are included in further analyses due to augmented correlation coefficients ($\Delta r > 0.02$) with Nix color variables when compared to Nix correlations with untransformed TC and TC stock variables. In general, Lab *a*, LCh *h*, and CMYK Y_K displayed the lowest correlations with soil carbon. Conversely, correlation coefficients with Ln(TC) exceeded 0.70 ± 0.02 in magnitude for six Nix color variables: Lab (1) *L*, XYZ (2) *X* and (3) *Y*, RGB (4) *R* and (5) *G*, and CMYK (6) K_K ($|r| > 0.68$; $p < 0.01$; Table 3). *X* and *Y* from the XYZ color space, as well as *R* and *G* from the RGB color space, showed high collinearity, respectively ($|r| \geq 0.90$; see Schmidt and Ahn, 2021). From the XYZ space, *X* was selected over *Y* as a final Nix color variable to avoid confusion between *Y* and Y_K (yellow) from the CMYK color space. Despite the lack of one-to-one relationship between RGB *R* and the hue red, *R* (red) was selected over *G* (green) as the best estimate of Ln(TC) from the RGB color space because of the perceptible relationship between soil redness and oxidized irons as well as hydrology (Schwertmann, 1993; Schwertmann and Taylor, 1989; Viscarra Rossel et al., 2006). Since Ln(TC) has been used in previous research using the Nix (Mikhailova et al., 2017; Mukhopadhyay et al., 2020; Mukhopadhyay and Chakraborty, 2020; Stiglitz et al., 2017) and no Nix–TC (%) correlations exceeded 0.70 in magnitude (Table 3), Ln (TC) was selected as the final carbon variable for regression analyses. The final four Nix color variables were thus *L* (CIE–Lab), *X* (XYZ), *R* (RGB), and K_K (CMYK).

Table 3
Pearson correlation coefficients between Nix color variables (n = 15) and soil carbon variables (TC [%], TC stocks [kg•m^{-2}], Ln[TC], and Ln([TC stocks]).

Nix Color Variables	TC (%)	TC Stocks (kg•m^{-2})	Ln(TC)	Ln(TC Stocks)
Lab				
L [a]	−0.64	−0.58	−0.70 [c]	*−0.65*
A	−0.24	−0.11	−0.21	−0.13
B	−0.52	−0.42	−0.61	−0.53
LCh				
C	−0.50	−0.39	−0.58	−0.49
H	−0.19	−0.21	−0.29	−0.29
XYZ				
X [a]	−0.61	−0.56	−0.70	*−0.65*
Y	−0.61	−0.57	*−0.69* [b]	*−0.65*
Z	−0.59	−0.57	*−0.65*	−0.62
RGB				
R [a]	−0.64	−0.57	−0.70	−0.64
G	−0.63	−0.58	−0.70	*−0.65*
B	−0.61	−0.58	*−0.66*	−0.62
CMYK				
C_K	0.58	0.48	0.64	0.56
M_K	0.55	0.54	0.64	0.61
Y_K	0.28	0.37	0.26	0.31
K_K [a]	*0.65*	0.59	0.70	*0.65*

*Note: all correlations where $|r| > 0.30$ are statistically significant ($p < 0.01$).
[a] Denotes Nix variables with $|r| \geq 0.70$ for at least one carbon variable (excluding G, as explained in the methods [Section 2.4] and results [Section 3.3]).
[b] *Italics*: $0.70 > |r| \geq 0.65$.
[c] Underline: $|r| \geq 0.70$.

3.3. Linear regressions models

Regression models conducted using the aggregate dataset for Ln(TC) versus final Nix color variables (*L*, *X*, *R*, and K_K) are displayed in Fig. 2. Simple linear regressions between final Nix color variables and Ln(TC) produced adequate models, where $R^2 = 0.50$ for Ln(TC) versus Lab L and RGB *R*, and $R^2 = 0.49$ for Ln(TC) versus XYZ *X* and CMYK K_K, respectively ($p < 0.01$ for all). Residual analyses indicated that models tended to overestimate soil carbon for lower values of Ln(TC) (e.g., Ln[TC] < −5) and underestimate soil carbon for higher values of Ln(TC) (e.g., Ln [TC] > −3.5), with nonnormal residuals (Fig. 2). High spread in Nix color measurements for individual carbon contents (i.e., at a given plot and depth interval)—visualized as horizontal spread in Fig. 2—decreased each model's explanatory power. Nonetheless, residuals tended to show homoscedasticity, and R^2 values that approximate 0.50 highlight the capacity for simple linear regressions to explain a significant portion of Ln(TC) variability.

When Nix–Ln(TC) coordinate pairs were separated by factor levels of physiography (Piedmont, Coastal Plain), regression model slopes and strengths were affected. Coastal Plain, but not Piedmont, regressions were significant; R^2 values surpassed those achieved using from the aggregate dataset and ranged from 0.55 (K_K) to 0.65 (*R*) ($p < 0.05$; Fig. 2; Table 4). In contrast, Piedmont regressions were weak and insignificant ($p > 0.25$).

When color measurements for final Nix variables were first averaged by plot and depth interval (i.e., all colors measured for a given carbon content), averaged colors could explain roughly 70% of the variability in Ln(TC), with R^2 ranging from 0.66 (K_K) to 0.70 (*R*) (Fig. 3; $p < 0.01$ for all). Comparisons between these regression strengths (Fig. 3) and those obtained from each individual color scan (Fig. 2) suggest that obtaining average color data for all sizeable colors observed at a given depth can provide more reliable estimates of TC than individual color measurements. Furthermore, regression slopes—a sign of model sensitivity—were 40–55% higher for averaged data (Fig. 3) than aggregate data (Fig. 2) (*L*: −0.07 vs. −0.049; *X*: −0.12 vs. −0.08; *R*: −0.03 vs. −0.02; K_K: 4.50 vs. 3.19, respectively), suggesting averaged data models are both more robust sensitive to changes in soil carbon.

Finally, the multiple linear regression model revealed that the use of multiple variables recorded by the Nix—*a* (Lab), *Y* (XYZ), *B* (RGB), and all variables of the CMYK color space (C_K, M_K, Y_K, and K_K)—can be used to estimate Ln[TC] with an adjusted R^2 of 0.60, per the following equation ($p < 0.01$):

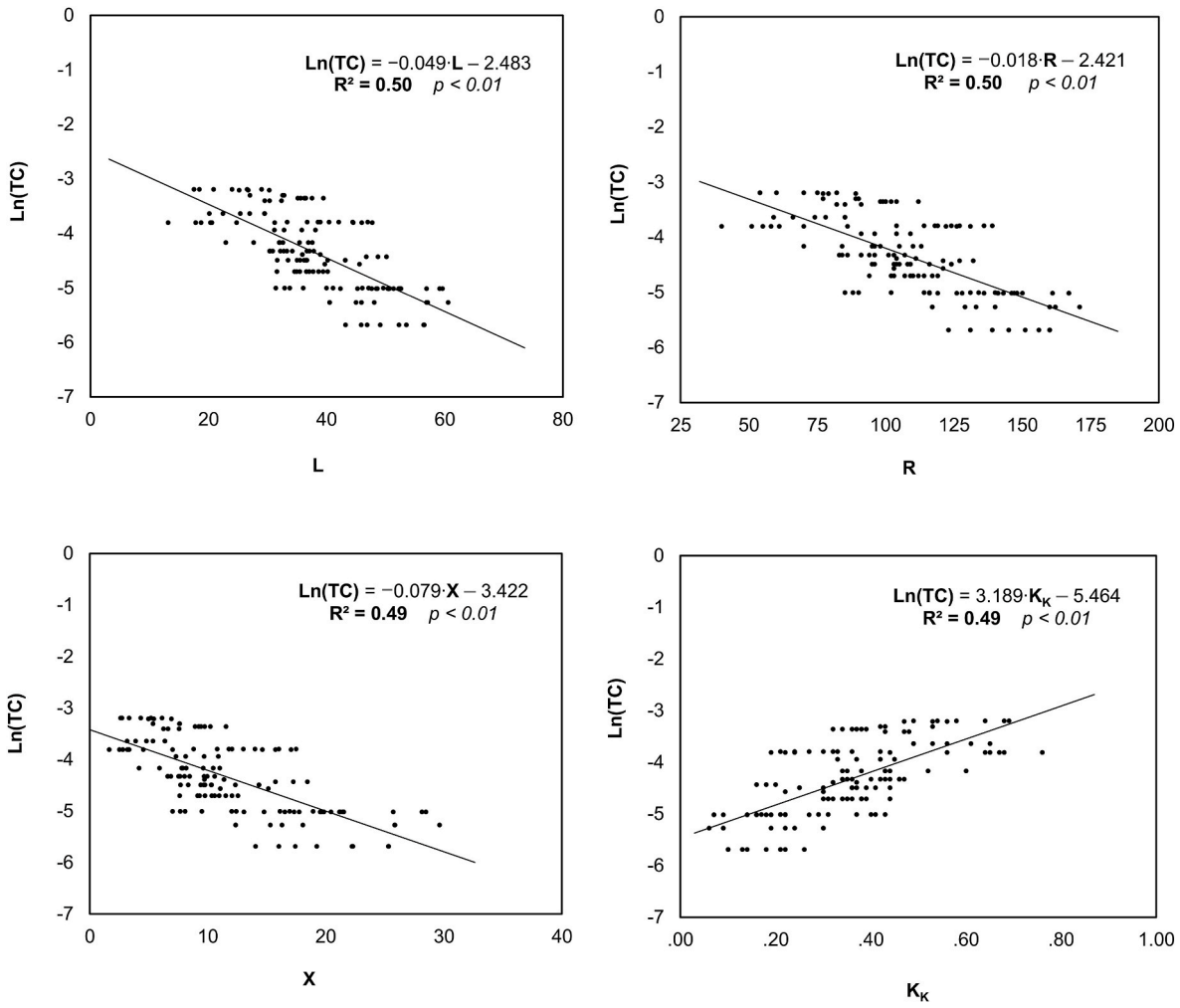

Fig. 2. Regressions for the natural log of soil carbon, Ln(TC), versus final Nix color variables (L, X, R, and K_K), using coordinate pairs from the aggregate dataset (n = 134) that includes all measured colors and soil carbon contents/stocks for all plots and respective depth intervals (0–10, 10–20, and 20–30 cm).

$$Ln(TC) = 0.431 \cdot a - 0.172 \cdot Y + 0.326 \cdot B + 14.314 \cdot C_K - 20.274 \cdot M_K + 37.070 \cdot Y_K + 31.055 \cdot K_K - 54.525 \quad \text{(Eq.1)}$$

Statistical analysis indicated that Lab a, RGB B, and CMYK Y_K and K_K were most significant ($p < 0.01$); furthermore, standardized beta coefficients were highest in magnitude for Lab B (7.654) and CMYK K_K (6.804). Fig. 4 displays predicted versus observed TC (%) derived from Equation (1). Residuals were not independently distributed, and the model tended to underestimate TC for low-carbon soils (observed TC < 1.5%) and overestimate TC where observed TC exceeded 3%.

4. Discussion

4.1. Nix colors and soil carbon

Nix measurements can highlight sitewide differences in colors that may reflect their differences in soil carbon contents and stocks. Variables like Lab L and CMYK K_K indicated color differences between (1) BR and JJM and (2) ARP and MN that mirrored differences in carbon contents and stocks (Section 3.1; Table 2). When soil carbon comparison rather than prediction is a management or outreach goal, simple comparisons between these Nix color variables may be suitable. Including more sites with varied soil colors and carbon contents would improve the understanding of how the Nix may be used as a carbon comparison tool. Furthermore, certain Nix color variables can be useful for identifying signatures of soil settings that are inexorably linked to soil carbon content—e.g., parent material, physiography, hydrology, and soil biogeochemistry. While the number of study sites was limited in this investigation, differences between Coastal Plain and Piedmont soil colors highlighted through the hue-related variables Lab a and LCh h likely relate to iron oxide contents that are known to differ between the physiographic provinces (Rossi and Rabenhorst, 2016). Furthermore, the large spread, high values for XYZ X and RGB R, and low values for CMYK K_K at MN might signal the prevalence of depleted (light, low-chroma) soil matrices as well as redox concentrations that were most abundant at MN (Ahn et al., 2009). As soil color determinations are a primary to indicate hydrologic and soil biogeochemical settings, significant differences in variables like CMYK K_K—related to both soil moisture and organic matter content—between sites highlight the potential for the Nix to be further investigated for the purpose of hydric soil delineation (USDA—NRCS, 2018).

The distributions of Nix soil color variables presented herein add to

Table 4
Regression model equations and R^2 values for the natural log of soil carbon, Ln (TC), versus final Nix color variables (L, X, R, and K_K), when separated by physiographic province (Piedmont vs. Coastal Plain).

Nix Color Variable	*Physiographic Province*	
	Piedmont	Coastal Plain
L		
R^2	0.05	**0.62**
p-value	>0.25	**0.00****
β (slope)	−0.219	−0.05
Intercept	1.273	2.061
X		
R^2	0.04	**0.60**
p-value	> 0.25	**0.00****
β (slope)	−0.036	−0.082
Intercept	0.844	1.159
R		
R^2	0.05	**0.65**
p-value	> 0.25	**0.00** **
β (slope)	−0.008	−0.018
Intercept	1.315	2.127
K_K		
R^2	0.05	**0.55**
p-value	> 0.25	**0.00** **
β (slope)	1.457	2.909
Intercept	0.056	0.939

*italics: p < 0.05.
**bold: p < 0.01.

the potential ranges for Nix color variables successfully used to discern color relationships with soil carbon. Compared to Stiglitz et al. (2016), the 134 data color measurements of this study included higher ranges for M_K (0.41–0.67 versus 0.31–0.41) and Y_K (0.63–0.83 versus 0.55–0.66), and a wider range for K_K (0.06–0.76 versus 0.55–0.66); these discrepancies may stem from differences in climate, geography, presence/absence of hydric soils, or differences in methodology (i.e., on-site color determinations versus sample processing before color determinations). Color variable ranges for these Piedmont and Coastal Plain soils were comparable to colors that can be observed on the global scale, but ranges for variables like Lab *a* and *b,* LCh *C* and *h,* and RGB *B* were relatively small (Viscarra Rossel et al., 2006).

With respect to soil carbon, forested wetlands in areas with similar landcover patterns have been documented to host carbon stocks of 10–14 kg m^{-2} (Bae and Ryu, 2015; Nave et al., 2019). While this research identified carbon stocks that were at most 5.7 kg m^{-2}, ranges reported herein for soil carbon (Section 3.1) are similar to those reported for forested wetlands within the Mid-Atlantic Piedmont and Coastal Plain physiographic provinces, with common reports of carbon contents ranging from 0.7% to 4.1% up to a depth of 15 cm (Ahn and Peralta, 2012; D'Angelo et al., 2005; Dee and Ahn, 2012; NOE, 2011; Stolt et al., 2000); thus, this study provides sufficient variability in soil carbon for assessing sitewide differences between, and relationships with, Nix color variables.

4.2. Relationships between color and carbon in forested wetland soils

Previous research has unearthed strong relationships between soil color and both carbon contents (Aitkenhead et al., 2015; Chen et al., 2018; Ibáñez-Asensio et al., 2013; Liles et al., 2013; Mikhailova et al., 2017; Pretorius et al., 2017; Schulze et al., 1993; Wills et al., 2007) and carbon stocks (Chaplot et al., 2001; Konen et al., 2003; Moritsuka et al., 2014; Viscarra Rossel et al., 2006; Wills et al., 2007), where many studies based the choice of TC versus TC stocks on application and/or audience rather than regression strengths. The finding herein that Nix

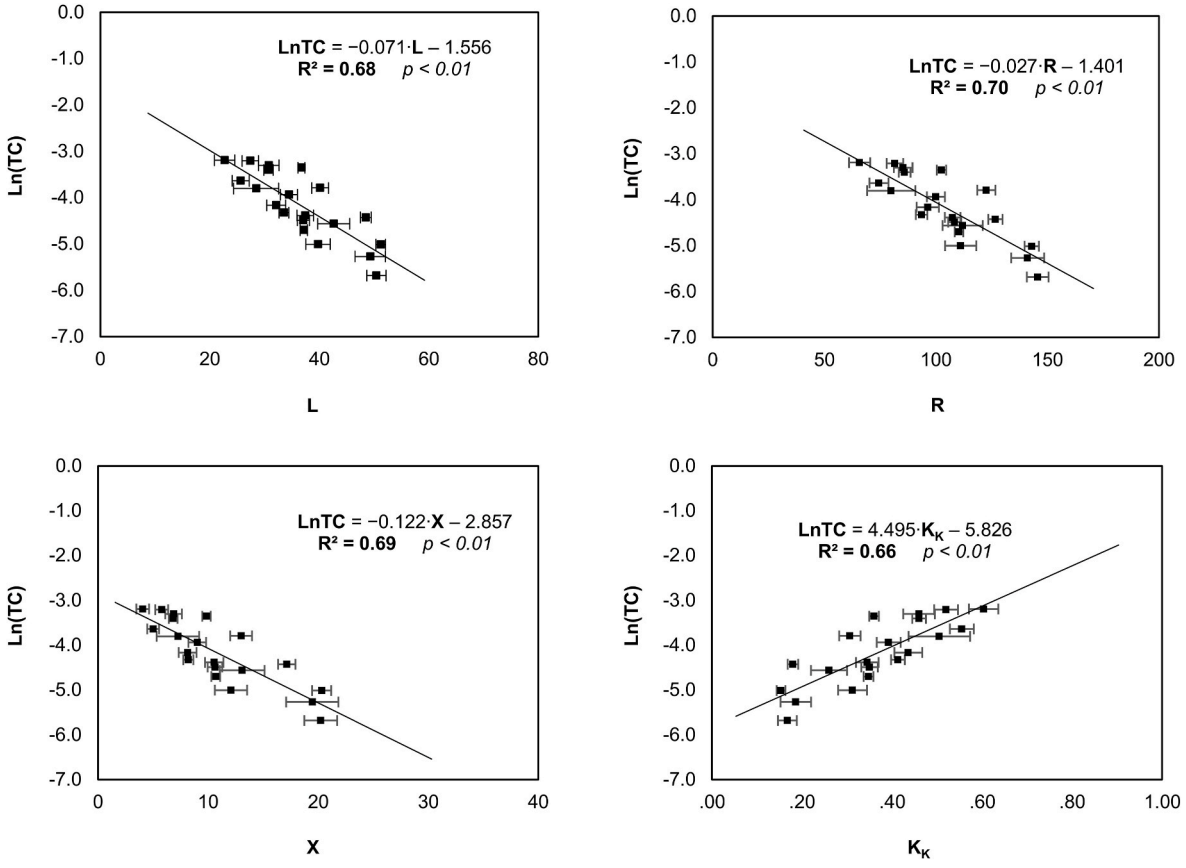

Fig. 3. Regressions for the natural log of soil total carbon (i.e.,Ln[TC]) versus final Nix color variables (L, X, R, and K_K), using coordinate pairs from averaged data that includes one averaged color measurement per soil carbon content at each plot and depth interval ($p < 0.01$ for all).

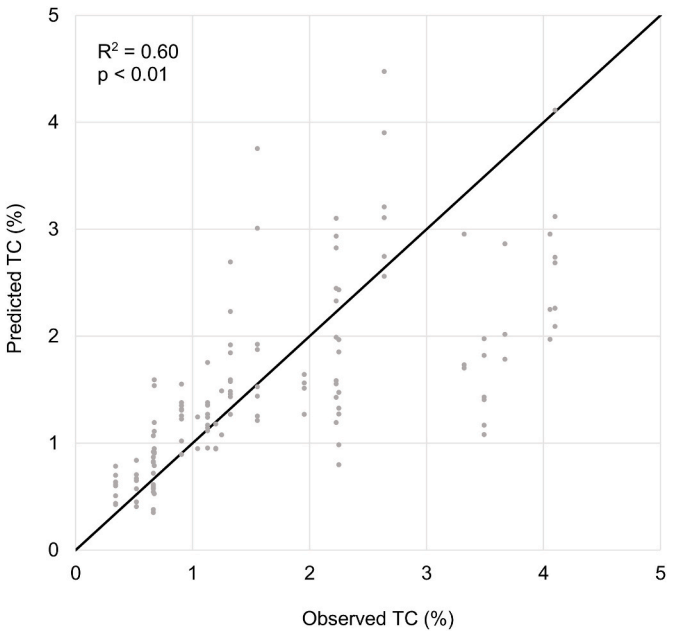

Fig. 4. Predicted versus observed TC (n = 134) obtained from the multiple linear regression (MLR) model using Nix variables *a*, *Y*, *B*, C_K, M_K, Y_K, and K_K; i.e., Predicted Ln(TC) = 0.431•*a* – 0.172•*Y* + 0.326 *B* + 14.314•C_K – 20.274•M_K + 37.070•Y_K + 31.055•K_K – 54.525 (R^2 = 0.60).

color variables are more highly correlated with TC than TC stocks may be inherent to color–carbon relationships, indicating that predictions of soil carbon from Nix color variables may not require further soil physicochemical analyses—e.g., measurement of D_b (Wills et al., 2007). Furthermore, the choice to transform TC using a natural logarithm is both present (Mikhailova et al., 2017; Stiglitz et al., 2018) and absent (Mukhopadhyay et al., 2020) in literature using the Nix. Mukhopadhyay et al. (2020) found a relatively high correlation between Nix variables and SOC (%) as opposed to Ln(SOC); however, an apparent nonrandom residual pattern in their scatterplot gives credence to the conclusion that soil carbon is linearly correlated with variables of soil color after undergoing a log transformation, these results extend that conclusion to soil color as measured in the field. Despite Fig. 2 revealing nonrandom residual patterns for all four scatterplots—particularly for Ln(TC) vs. L—the Ln(TC) function provided the best residual pattern out of TC and the common transformations explored in this study (square root [$\sqrt{x}$] and inverse [x^{-1}]). It is recommended that the Nix be used to assess color—carbon relationships with soils that provide a higher range of carbon contents to more thoroughly assess the linearity of Ln(TC) vs. Nix color variable models.

Using Ln(TC) as a proxy for soil carbon, soil carbon can be best predicted using Nix color variables *L*, *X*, *R*, and K_K with moderately strong coefficients of determination ($R^2 \approx 0.50$), deemed to be acceptable by this study's standards ($|r| \geq 0.70$ and $R^2 \geq 0.49$; Table 3; Fig. 2). In contrast to a single variable solution, these four variables are offered to allow flexibility in color space choice (CIE–Lab, XYZ, RGB, and/or CMYK). However, compared to XYZ *X* and CMYK K_K, variables *L* (Lab) and *R* (RGB) have slightly higher R^2 values (0.50 versus 0.49; $p < 0.01$), more randomness in residual patterns, and larger y-intercepts (−2.483 [*L*] and −2.421 [*R*] versus −3.422 [*X*] and −5.464 [*Y*]) that more adequately estimate soil carbon contents when soil color approaches black (Fig. 2). Similar results were observed in previous studies, as soil lightness—i.e., Lab *L*—and SOC have been prominently linked (e.g., r = −0.74 in Viscarra Rossel et al., 2006) with a linear or curvilinear relationship (Brown and O'Neal, 1923; Konen et al., 2003; Liles et al., 2013; Mikhailova et al., 2017; Moritsuka et al., 2014; Pretorius et al., 2017; Schulze et al., 1993; Stiglitz et al., 2017, 2018; Wills et al., 2007; Yang et al., 2001; Yonekura et al., 2010). Furthermore, strong correlations between soil carbon and RGB *R* (r = −0.79) have also been identified (Viscarra Rossel et al., 2006; Ibáñez-Asensio et al., 2013).

This study's results corroborated the finding that distinct soil taxonomic and/or landscape settings can produce distinct regression models and strengths (e.g., for *L*: R^2 = 0.62 for Coastal Plain soils [Table 4] vs. R^2 = 0.50 for all soils from both Coastal Plain and Piedmont [Fig. 2]; $p < 0.01$ for both). Nix color measurements may thus be more useful if models are confined to a limited soilscape (Ibáñez-Asensio et al., 2013; Mikhailova et al., 2017; Moritsuka et al., 2014; Stiglitz et al., 2018; Valeeva et al., 2016; Viscarra Rossel et al., 2006; Wills et al., 2007). Unlike Coastal Plain soils, Piedmont soils fall within the Culpeper Triassic Basin and have higher clay and iron oxide contents, which provide abundant binding sites for soil organic carbon. Carbon physicochemistry and resulting color patterns are inherently different in the Piedmont than in the Coastal Plain (Adhikari and Yang, 2015; Elless et al., 1996). Furthermore, soil carbon has a stronger monotonic (curvi-) linear relationship with sand content than clay content (Baldock and Skjemstad, 2000; Six et al., 2002; Torn et al., 1997; van Breemen and Feijtel, 1990; Wills et al., 2007), and Coastal Plain soils are generally sandier (Markewich et al., 1990). In accordance with previous studies, this research highlights that accurate models for soil carbon estimation from soil color measurements should be constrained to specific mineralogical and physiographic settings with less obfuscation from high clay contents.

Stronger R^2 values for Nix−carbon regression models reliant on averaged rather than aggregate data suggests that multiple color measurements for the same soil depth should be averaged when creating carbon regression models. While such averaging requires more sampling and temporal engagement, it bolsters the applications of using color over time to track carbon changes and provide management opportunities to improve wetland carbon storage. Finally, in contrast to previous studies obtaining high (>0.90) R^2 values when models were based on Lab L, *a*, and/or *b*, this study's MLR analysis rendered a model able to explain 60% of the variation in Ln(TC) in which *L* was excluded ($p \approx 0.25$) and RGB *B* and CMYK K_K were the strongest predictors (Equation (1)). The influence of RGB *B*—which had a Pearson correlation coefficient of −0.66 with Ln(TC) (Table 3)—signals that, despite the link between soil color and additive blue, RGB *B* offers additional information than offered through soil lightness (L, K_K) alone. The MLR nonetheless could not predict Ln(TC) to the extent of average color measurements of *L*, *X*, *R*, or K_K alone (Fig. 3). As shown in Fig. 4, the model tended to underestimate TC for soils with high TC (>2.5%), bolstering the recommendation that multiple color measurements be taken and averaged when creating and relying on linear regression models.

4.3. Implications and limitations of the study

The applications of these findings rest upon the on-site nature of color measurements and the accuracy of model predictions. This study is one of the first linking quantitative soil color variables and carbon contents to occur on-site using non-processed samples (see Wills et al., 2007 for others), but the confirmation of relationships between Nix color variables and soil carbon were met with relatively large deviations in regression models (>1 difference in Ln[TC]) with a substantial variance in Ln(TC) left unexplained. Simple linear regressions of Ln(TC) versus Nix variables like *L* may improve with procedural improvements that control for confounding variables like soil moisture, texture, and surface evenness (Stiglitz et al., 2016; Wu et al., 2009). Nonetheless, complete control cannot be attained in a field setting, and it remains to be seen if regression strengths observed in lab studies like Chen et al. (2018; R^2 = 0.71), Viscarra Rossel et al. (2006; R^2 = 0.76), and Mikhailova et al. (2017; R^2 = −0.87) can be achieved in on-site color determinations and carbon estimations. Particularly when using the Nix to forested wetland areas known to contain iron and/or manganese redoximorphic features, heterogeneous color patterns in the soil matrix can complicate the applicability of such regression models by

obfuscating the relationship between soil color and carbon contents. Demonstrated through a comparison of R^2 and overall scatter between regression models based on aggregate versus averaged datasets (Figs. 2 and 3), it is recommended that users average Nix color variable values at a certain depth (e.g., $[K_{K(1)} + K_{K(2)}]/2$) when more than one significant color is identified in a soil horizon, and to ignore insubstantial features like concentrations comprising less than 25% of the soil matrix.

Beyond quality control concerns, studies have identified additional variables affecting regression models that may warrant further study for field-based investigations. For example, depth is known to affect the relationship between soil color and soil carbon; while soil colors were matched to each respective depth interval's carbon contents in this study, previous investigations have gone one step further to incorporate depth into their models as an auxiliary variable (Mikhailova et al., 2017; Stiglitz et al., 2017, 2018; Wills et al., 2007). This is a promising approach if studies incorporate sufficient sampling points into their analysis, but also complicates model accessibility. Similar to the suggestions of Mukhopadhyay et al. (2020), it is recommended that quality control efforts focus on controlling other variables to augment correlation and regression strengths rather than relying on an additional input for regression models.

5. Conclusions

The outcome of the study demonstrates that field deployment of the Nix Color Sensor and accompanying app has the potential to not only differentiate soils of contrasting colors and carbon contents, but also predict soil carbon contents through a simple linear regression equation providing an estimate of Ln(TC). Nix color variables—notably L (Lab), X (XYZ), R (RGB), and K_K (CMYK)—were more capable of predicting Ln (TC) in certain physiographic settings, specifically the Coastal Plain, highlighting that refinement of Nix methodologies may be required on a regionally-specific scale. Independent of physicochemical properties, however, it is suggested that investigations into, and/or application of, the Nix as a tool for soil carbon prediction focus on soils within a uniform landscape and with reliance on averaged matrix color measurements.

Unlike the MSCC or more expensive methods, the Nix has the potential to be accessibly integrated into carbon storage and sequestration strategies that would benefit from accurate, relatively inexpensive, and sustained efforts, along with simple statistical models, to predict soil carbon at promising carbon sinks like forested wetlands. While further research is warranted to better understand color–carbon relationships in soils within different physiographic provinces as well as ecosystem types, these findings offer an optimistic basis for potentially incorporating the Nix and its soil color measurements into environmental monitoring and assessments, carbon-focused watershed management, and/or soil science education and training.

Funding source

This research did not receive any specific grant from funding agencies in the public, commercial, or not-for-profit sectors.

Author contributions

Stephanie A Schmidt: Data Collection (Field work), Data Analysis, Writing – Original draft preparation. **Changwoo Ahn:** Conceptualization (Design of the study), Supervision, Data Analysis, Writing – Reviewing, Editing and Rewriting.

Declaration of competing interest

The authors declare that they have no known competing financial interests or personal relationships that could have appeared to influence the work reported in this paper.

Acknowledgments

The authors thank Katie Ledford and Jesse Wong for their help with field work and Katie Ledford and Katrina Napora for their assistance with soil processing and carbon analysis.

References

Adhikari, D., Yang, Y., 2015. Selective stabilization of aliphatic organic carbon by iron oxide. Sci. Rep. 5, 11214. https://doi.org/10.1038/srep11214.
Ahn, C., Gillevet, P.M., Sikaroodi, M., Wolf, K.L., 2009. An assessment of soil bacterial community structure and physicochemistry in two microtopographic locations of a palustrine forested wetland. Wetl. Ecol. Manag. 17, 397–407. https://doi.org/10.1007/s11273-008-9116-4.
Ahn, C., Jones, S., 2013. Assessing organic matter and organic carbon contents in soils of created mitigation wetlands in Virginia. Environ. Eng. Res. 18, 151–156. https://doi.org/10.4491/eer.2013.18.3.151.
Ahn, C., Peralta, R.M., 2012. Soil properties are useful to examine denitrification function development in created mitigation wetlands. Ecol. Eng. 49, 130–136. https://doi.org/10.1016/j.ecoleng.2012.08.039.
Aitkenhead, M.J., Donnelly, D., Sutherland, L., Miller, D.G., Coull, M.C., Black, H.I.J., 2015. Predicting Scottish topsoil organic matter content from colour and environmental factors. Eur. J. Soil Sci. 66, 112–120. https://doi.org/10.1111/ejss.12199.
Akoglu, H., 2018. User's guide to correlation coefficients. Turkish J. Emer. Med. 18, 91–93. https://doi.org/10.1016/j.tjem.2018.08.001.
Bae, J., Ryu, Y., 2015. Land use and land cover changes explain spatial and temporal variations of the soil organic carbon stocks in a constructed urban park. Landsc. Urban Plann. 136, 57–67. https://doi.org/10.1016/j.landurbplan.2014.11.015.
Baldock, J.A., Skjemstad, J.O., 2000. Role of the soil matrix and minerals in protecting natural organic materials against biological attack. Org. Geochem. 31, 697–710. https://doi.org/10.1016/S0146-6380(00)00049-8.
Becker, T.E., Robertson, M.M., Vandenberg, R.J., 2019. Nonlinear transformations in organizational research: possible problems and potential solutions. Organ. Res. Methods 22, 831–866. https://doi.org/10.1177/1094428118775205.
Bernal, B., Mitsch, W.J., 2013. Carbon sequestration in two created riverine wetlands in the Midwestern United States. J. Environ. Qual. 42, 1236–1244. https://doi.org/10.2134/jeq2012.0229.
Bishel-Machung, L., Brooks, R.P., Yates, S.S., Hoover, K.L., 1996. Soil properties of reference wetlands and wetland creation projects in Pennsylvania. Wetlands 16, 532–541. https://doi.org/10.1007/BF03161343.
Bossio, D.A., Cook-Patton, S.C., Ellis, P.W., Fargione, J., Sanderman, J., Smith, P., Wood, S., Zomer, R.J., von Unger, M., Emmer, I.M., Griscom, B.W., 2020. The role of soil carbon in natural climate solutions. Nat. Sustain. 3, 391–398. https://doi.org/10.1038/s41893-020-0491-z.
Bridgham, S.D., Megonigal, J.P., Keller, J.K., Bliss, N.B., Trettin, C., 2006. The carbon balance of North American wetlands. Wetlands 26, 889–916. https://doi.org/10.1672/0277-5212(2006)26[889. TCBONA]2.0.CO;2.
Brown, P., O'Neal, A., 1923. The color of soils in relation to organic matter content. Iowa Agric. Home Econ. Exp. Stn. Res. Bull. 5, 273–300.
Caldwell, P.V., Adams, A.A., Niewoehner, C.P., Vepraskas, M.J., Gregory, J.D., 2005. Sampling device to extract intact cores in saturated organic soils. Soil Sci. Soc. Am. J. 69, 2071–2075. https://doi.org/10.2136/sssaj2005.0150.
Chaplot, V., Bernoux, M., Walter, C., Curmi, P., Herpin, U., 2001. Soil carbon storage prediction in temperate hydromorphic soils using a morphologic index and digital elevation model. Soil Sci. 166, 48–60. https://doi.org/10.1097/00010694-200101000-00008.
Chen, Y., Zhang, M., Fan, D., Fan, K., Wang, X., 2018. Linear regression between CIE-Lab color parameters and organic matter in soils of tea plantations. Eurasian Soil Sci. 51, 199–203. https://doi.org/10.1134/S1064229318020011.
Chi, Y., Zheng, W., Shi, H., Sun, J., Fu, Z., 2018. Spatial heterogeneity of estuarine wetland ecosystem health influenced by complex natural and anthropogenic factors. Sci. Total Environ. 634, 1445–1462. https://doi.org/10.1016/j.scitotenv.2018.04.085.
Chimner, R.A., Ewel, K.C., 2005. A tropical freshwater wetland: II. Production, decomposition, and peat formation. Wetl. Ecol. Manag. 13, 671–684. https://doi.org/10.1007/s11273-005-0965-9.
D', Angelo, E., Karathanasis, A., Sparks, E., Ritchey, S., Wehr-McChesney, S., 2005. Soil carbon and microbial communities at mitigated and late successional bottomland forest wetlands. Wetlands 25, 162–175. https://doi.org/10.1672/0277-5212(2005)025[0162:SCAMCA]2.0.CO;2.
Dancey, C.P., Reidy, J., 2007. Statistics without Maths for Psychology. Pearson Education/Prentice Hall, p. 619.
Dee, S.M., Ahn, C., 2012. Soil properties predict plant community development of mitigation wetlands created in the Virginia Piedmont, USA. Environ. Manag. 49, 1022–1036. https://doi.org/10.1007/s00267-012-9838-1.
Elless, M.P., Rabenhorst, M.C., James, B.R., 1996. Redoximorphic features in soils of the triassic culpeper basin. Soil Sci. 161, 58–69. https://doi.org/10.1097/00010694-199601000-00008.
Elliot, A.J., 2015. Color and psychological functioning: a review of theoretical and empirical work. Front. Psychol. 6, 368.
Fan, Z., Herrick, J.E., Saltzman, R., Matteis, C., Yudina, A., Nocella, N., Crawford, E., Parker, R., Van Zee, J., 2017. Measurement of soil color: a comparison between

smartphone camera and the Munsell Color Charts. Soil Sci. Soc. Am. J. 81, 1139–1146. https://doi.org/10.2136/sssaj2017.01.0009.
Giannopoulos, G., Lee, D.Y., Neubauer, S.C., Brown, B.L., Franklin, R.B., 2019. A simple and effective sampler to collect undisturbed cores from tidal marshes. bioRxiv 515825. https://doi.org/10.1101/515825.
Giese, L., Flannagan, C., 2006. Soil properties in Northern Virginia created forested wetlands. In: Hydrology and Management of Forested Wetlands, Proceedings of the International Conference, April 8-12, 2006, New Bern, North Carolina, American Society of Agricultural and Biological Engineers. https://doi.org/10.13031/2013.20295.
Giese, L.A., Aust, W.M., Trettin, C.C., Kolka, R.K., 2000. Spatial and temporal patterns of carbon storage and species richness in three South Carolina coastal plain riparian forests. Ecol. Eng. 15, S157–S170. https://doi.org/10.1016/S0925-8574(99)00081-6.
Gómez-Robledo, L., López-Ruiz, N., Melgosa, M., Palma, A.J., Capitán-Vallvey, L.F., Sánchez-Marañón, M., 2013. Using the mobile phone as Munsell soil-colour sensor: an experiment under controlled illumination conditions. Comput. Electron. Agric. 99, 200–208. https://doi.org/10.1016/j.compag.2013.10.002.
Guo, L.B., Gifford, R.M., 2002. Soil carbon stocks and land use change: a meta analysis. Global Change Biol. 8, 345–360. https://doi.org/10.1046/j.1354-1013.2002.00486.x.
Han, P., Dong, D., Zhao, X., Jiao, L., Lang, Y., 2016. A smartphone-based soil color sensor: for soil type classification. Comput. Electron. Agric. 123, 232–241. https://doi.org/10.1016/j.compag.2016.02.024.
Ibáñez-Asensio, S., Marqués-Mateu, A., Moreno-Ramón, H., Balasch, S., 2013. Statistical relationships between soil colour and soil attributes in semiarid areas. Biosyst. Eng. 116, 120–129. https://doi.org/10.1016/j.biosystemseng.2013.07.013.
Jobbágy, E.G., Jackson, R.B., 2000. The vertical distribution of soil organic carbon and its relation to climate and vegetation. Ecol. Appl. 10, 423–436. https://doi.org/10.1890/1051-0761(2000)010[0423:TVDOSO]2.0.CO, 2.
Johansson, T., Malmer, N., Crill, P.M., Friborg, T., Åkerman, J.H., Mastepanov, M., Christensen, T.R., 2006. Decadal vegetation changes in a northern peatland, greenhouse gas fluxes and net radiative forcing. Global Change Biol. 12, 2352–2369. https://doi.org/10.1111/j.1365-2486.2006.01267.x.
Kirillova, N., Vodyanitskii, Y.N., Sileva, T., 2015. Conversion of soil color parameters from the Munsell system to the CIE-L* a* b* system. Eurasian Soil Sci. 48, 468–475.
Köchy, M., Hiederer, R., Freibauer, A., 2015. Global distribution of soil organic carbon – Part 1: masses and frequency distributions of SOC stocks for the tropics, permafrost regions, wetlands, and the world. SOIL 1, 351–365. https://doi.org/10.5194/soil-1-351-2015.
Konen, M.E., Burras, C.L., Sandor, J.A., 2003. Organic carbon, texture, and quantitative color measurement relationships for cultivated soils in North Central Iowa. Soil Sci. Soc. Am. J. 67, 1823–1830. https://doi.org/10.2136/sssaj2003.1823.
Lees, K.J., Quaife, T., Artz, R.R.E., Khomik, M., Clark, J.M., 2018. Potential for using remote sensing to estimate carbon fluxes across northern peatlands – a review. Sci. Total Environ. 615, 857–874. https://doi.org/10.1016/j.scitotenv.2017.09.103.
Liles, G.C., Beaudette, D.E., O'Geen, A.T., Horwath, W.R., 2013. Developing predictive soil C models for soils using quantitative color measurements. Soil Sci. Soc. Am. J. 77, 2173–2181. https://doi.org/10.2136/sssaj2013.02.0057.
Markewich, H.W., Pavich, M.J., Buell, G.R., 1990. Contrasting soils and landscapes of the Piedmont and Coastal Plain, eastern United States. Geomorphology. Proceedings of the 21st Annual Binghamton Symposium in Geomorphology 3, 417–447. https://doi.org/10.1016/0169-555X(90)90015-I.
Meersmans, J., Wesemael, B.V., Molle, M.V., 2009. Determining soil organic carbon for agricultural soils: a comparison between the Walkley & Black and the dry combustion methods (north Belgium). Soil Use Manag. 25, 346–353. https://doi.org/10.1111/j.1475-2743.2009.00242.x.
Menne, M.J., Durre, I., Korzeniewski, B., McNeill, S., Thomas, K., Yin, X., Anthony, S., Ray, R., Vose, R.S., Gleason, B.E., Houston, T.G., 2012. Global Historical Climatology Network - Daily (GHCN-Daily). https://doi.org/10.7289/V5D21VHZ. Version 3 [Daily Summaries].
Mikhailova, E.A., Stiglitz, R.Y., Post, C.J., Schlautman, M.A., Sharp, J.L., Gerard, P.D., 2017. Predicting soil organic carbon and total nitrogen in the Russian Chernozem from depth and wireless color sensor measurements. Eurasian Soil Sci. 50, 1414–1419. https://doi.org/10.1134/S106422931713004X.
Mitsch, W.J., Gosselink, J.G., 2015. Wetlands. John Wiley & Sons, Inc., Hoboken, New Jersey.
Moritsuka, N., Matsuoka, K., Katsura, K., Sano, S., Yanai, J., 2014. Soil color analysis for statistically estimating total carbon, total nitrogen and active iron contents in Japanese agricultural soils. Soil Sci. Plant Nutr. 60, 475–485.
Mukaka, M.M., 2012. Statistics corner: a guide to appropriate use of correlation coefficient in medical research. Malawi Med. J. 24, 69–71.
Mukhopadhyay, S., Chakraborty, S., 2020. Use of diffuse reflectance spectroscopy and Nix pro color sensor in combination for rapid prediction of soil organic carbon. Comput. Electron. Agric. 176, 105630. https://doi.org/10.1016/j.compag.2020.105630.
Mukhopadhyay, S., Chakraborty, S., Bhadoria, P.B.S., Li, B., Weindorf, D.C., 2020. Assessment of heavy metal and soil organic carbon by portable X-ray fluorescence spectrometry and NixPro™ sensor in landfill soils of India. Geoderma Regional 20, e00249. https://doi.org/10.1016/j.geodrs.2019.e00249.
Munsell, A.H., 1905. A Color Notation. G. H. Ellis Company, Boston, Massachusetts.
Nahlik, A.M., Fennessy, M.S., 2016. Carbon storage in US wetlands. Nat. Commun. 7, 13835. https://doi.org/10.1038/ncomms13835.
Nave, L.E., DeLyser, K., Butler-Leopold, P.R., Sprague, E., Daley, J., Swanston, C.W., 2019. Effects of land use and forest management on soil carbon in the ecoregions of Maryland and adjacent eastern United States. For. Ecol. Manag. 448, 34–47. https://doi.org/10.1016/j.foreco.2019.05.072.
Neitz, J., Carroll, J., Yamauchi, Y., Neitz, M., Williams, D.R., 2002. Color perception is mediated by a plastic neural mechanism that is adjustable in adults. Neuron 35, 783–792.
Noe, G.B., 2011. Measurement of net nitrogen and phosphorus mineralization in wetland soils using a modification of the resin-core technique. Soil Sci. Soc. Am. J. 75, 760–770. https://doi.org/10.2136/sssaj2010.0289.
O'Donnell, T.K., Goyne, K.W., Miles, R.J., Baffaut, C., Anderson, S.H., Sudduth, K.A., 2011. Determination of representative elementary areas for soil redoximorphic features identified by digital image processing. Geoderma 161, 138–146. https://doi.org/10.1016/j.geoderma.2010.12.011.
Pek, J., Wong, O., Wong, A., 2019. Data transformations for inference with linear regression: clarifications and recommendations. Practical Assess. Res. Eval. 22, 9. https://doi.org/10.7275/p86s-zc41.
Post, W.M., Izaurralde, R.C., Mann, L.K., Bliss, N., 2001. Monitoring and verifying changes of organic carbon in soil. In: Rosenberg, N.J., Izaurralde, R.C. (Eds.), Storing Carbon in Agricultural Soils: A Multi-Purpose Environmental Strategy. Springer Netherlands, Dordrecht, pp. 73–99. https://doi.org/10.1007/978-94-017-3089-1_4.
Pretorius, M., Huyssteen, C., Brown, L., 2017. Soil color indicates carbon and wetlands: developing a color-proxy for soil organic carbon and wetland boundaries on sandy coastal plains in South Africa. Environ. Monit. Assess. 189, 1–18. https://doi.org/10.1007/s10661-017-6249-z.
Pulighe, G., Fava, F., Lupia, F., 2016. Insights and opportunities from mapping ecosystem services of urban green spaces and potentials in planning. Ecosystem Services 22, 1–10. https://doi.org/10.1016/j.ecoser.2016.09.004.
Rawlins, B.G., Vane, C.H., Kim, A.W., Tye, A.M., Kemp, S.J., Bellamy, P.H., 2008. Methods for estimating types of soil organic carbon and their application to surveys of UK urban areas. Soil Use Manag. 24, 47–59. https://doi.org/10.1111/j.1475-2743.2007.00132.x.
Roper, W.R., Robarge, W.P., Osmond, D.L., Heitman, J.L., 2019. Comparing four methods of measuring soil organic matter in North Carolina soils. Soil Sci. Soc. Am. J. 83, 466–474. https://doi.org/10.2136/sssaj2018.03.0105.
Rossi, A.M., Rabenhorst, M.C., 2016. Pedogenesis and landscape relationships of a Holocene age barrier island. Geoderma 262, 71–84. https://doi.org/10.1016/j.geoderma.2015.08.004.
Sahoo, U.K., Singh, S.L., Gogoi, A., Kenye, A., Sahoo, S.S., 2019. Active and passive soil organic carbon pools as affected by different land use types in Mizoram, Northeast India. PloS One 14, e0219969. https://doi.org/10.1371/journal.pone.0219969.
Sánchez-Marañón, M., García, P.A., Huertas, R., Hernández-Andrés, J., Melgosa, M., 2011. Influence of natural daylight on soil color description: assessment using a color-appearance model. Soil Sci. Soc. Am. J. 75, 984–993.
Säynäjoki, E.S., Korba, P., Kalliala, E., Nuotio, A.K., 2018. GHG emissions reduction through urban planners' improved control over Earthworks: a case study in Finland. Sustainability 10, 2859. https://doi.org/10.3390/su10082859.
Schlesinger, W.H., 1990. Evidence from chronosequence studies for a low carbon-storage potential of soils. Nature 348, 232–234. https://doi.org/10.1038/348232a0.
Schmidt, S.A., Ahn, C., 2021. Analysis of soil color variables and their relationships between two field-based methods and its potential application for wetland soils. Sci. Total Environ. 783, 147005. https://doi.org/10.1016/j.scitotenv.2021.147005.
Schmidt, S.A., Ahn, C., 2019. A comparative review of methods of using soil colors and their patterns for wetland ecology and management. Commun. Soil Sci. Plant Anal. 50, 1293–1309. https://doi.org/10.1080/00103624.2019.1604737.
Schulze, D.G., Nagel, J.L., Scoyoc, G.E.V., Henderson, T.L., Baumgardner, M.F., Stott, D.E., 1993. Significance of organic matter in determining soil colors. In: Bigham, J.M., Ciolkosz, E.J. (Eds.), Soil Color. John Wiley & Sons, Ltd, pp. 71–90. https://doi.org/10.2136/sssaspecpub31.c5.
Schwertmann, U., 1993. Relations between iron oxides, soil color, and soil formation. In: Bigham, J.M., Ciolkosz, E.J. (Eds.), Soil Color. John Wiley & Sons, Ltd, pp. 51–69. https://doi.org/10.2136/sssaspecpub31.c4.
Schwertmann, U., Taylor, R.M., 1989. Iron oxides. In: Dixon, J.B., Weed, S.B. (Eds.), Minerals in Soil Environments. John Wiley & Sons, Ltd, pp. 379–438. https://doi.org/10.2136/sssabookser1.2ed.c8.
Six, J., Conant, R.T., Paul, E.A., Paustian, K., 2002. Stabilization mechanisms of soil organic matter: implications for C-saturation of soils. Plant Soil 241, 155–176. https://doi.org/10.1023/A:1016125726789.
Stiglitz, R.Y., Mikhailova, E., Post, C., Schlautman, M., Sharp, J., 2017. Using an inexpensive color sensor for rapid assessment of soil organic carbon. Geoderma 286, 98–103. https://doi.org/10.1016/j.geoderma.2016.10.027.
Stiglitz, R.Y., Mikhailova, E., Post, C., Schlautman, M., Sharp, J., 2016. Evaluation of an inexpensive sensor to measure soil color. Comput. Electron. Agric. 121, 141–148. https://doi.org/10.1016/j.compag.2015.11.014.
Stiglitz, R.Y., Mikhailova, E.A., Sharp, J.L., Post, C.J., Schlautman, M.A., Gerard, P.D., Cope, M.P., 2018. Predicting soil organic carbon and total nitrogen at the farm scale using quantitative color sensor measurements. Agronomy 8, 212. https://doi.org/10.3390/agronomy8100212.
Stolt, M.H., Genthner, M.H., Daniels, W.L., Groover, V.A., Nagle, S., Haering, K.C., 2000. Comparison of soil and other environmental conditions in constructed and adjacent palustrine reference wetlands. Wetlands 20, 671–683. https://doi.org/10.1672/0277-5212(2000)020[0671. COSAOE]2.0.CO;2.
Torn, M.S., Trumbore, S.E., Chadwick, O.A., Vitousek, P.M., Hendricks, D.M., 1997. Mineral control of soil organic carbon storage and turnover. Nature 389, 170–173. https://doi.org/10.1038/38260.
Torrent, J., Barrón, V., 1993. Laboratory measurement of soil color: theory and practice. In: Bingham, J.M., Ciolkosz, E.J. (Eds.), Soil Color. SSSA Special Publication No. 31, Madison, WI, pp. 21–33. https://doi.org/10.2136/sssaspecpub31.c2.

United States Department of Agriculture - Natural Resources Conservation Service [USDA - NRCS], 2018. Field Indicators of Hydric Soils in the United States, Version 8.2.

USDA–NRCS Soil Survey Staff, 2020. Web Soil Survey. Version 3.4.0. http://websoilsurvey.nrcs.usda.gov/app/WebSoilSurvey.aspx. (Accessed 5 July 2020).

Valeeva, A.A., Aleksandrova, A.B., Koposov, G.F., 2016. Color estimation of forest-steppe soils by digital photography under laboratory conditions. Eurasian Soil Sci. 49, 1033–1037. https://doi.org/10.1134/S1064229316090131.

van Breemen, N. van, Feijtel, T., 1990. Soil processes and properties involved in the production of greenhouse gases, with special relevance to soil taxonomic systems. In: Bouwman, A.F. (Ed.), Soils and the Greenhouse Effect. John Wiley & Sons Ltd., Chichester, pp. 195–223.

Villa, J.A., Bernal, B., 2018. Carbon sequestration in wetlands, from science to practice: an overview of the biogeochemical process, measurement methods, and policy framework. Ecol. Eng. Wet. Carbon Rev. 114, 115–128. https://doi.org/10.1016/j.ecoleng.2017.06.037.

Villa, J.A., Mitsch, W.J., 2015. Carbon sequestration in different wetland plant communities in the Big Cypress Swamp region of southwest Florida. Int. J. Biodiv. Sci. Ecosyst. Serv. Manag. 11, 17–28. https://doi.org/10.1080/21513732.2014.973909.

Virginia Department of Environmental Quality, 2019. Chesapeake Bay TMDL Phase III Watershed Implementation Plan (Richmond, Virginia).

Viscarra Rossel, R.A., Cattle, S.R., Ortega, A., Fouad, Y., 2009. In situ measurements of soil colour, mineral composition and clay content by vis–NIR spectroscopy. Geoderma 150, 253–266. https://doi.org/10.1016/j.geoderma.2009.01.025.

Viscarra Rossel, R.A., Minasny, B., Roudier, P., McBratney, A.B., 2006. Colour space models for soil science. Geoderma 133, 320–337. https://doi.org/10.1016/j.geoderma.2005.07.017.

Whiting, G.J., Chanton, J.P., 2001. Greenhouse carbon balance of wetlands: methane emission versus carbon sequestration. Tellus B 53, 521–528. https://doi.org/10.1034/j.1600-0889.2001.530501.x.

Wills, S.A., Burras, C.L., Sandor, J.A., 2007. Prediction of soil organic carbon content using field and laboratory measurements of soil color. Soil Sci. Soc. Am. J. 71, 380–388. https://doi.org/10.2136/sssaj2005.0384.

Wu, C.Y., Jacobson, A.R., Laba, M., Baveye, P.C., 2009. Accounting for surface roughness effects in the near-infrared reflectance sensing of soils. Geoderma 152, 171–180. https://doi.org/10.1016/j.geoderma.2009.06.002.

Xue, Z., Hou, G., Zhang, Z., Lyu, X., Jiang, M., Zou, Y., Shen, X., Wang, J., Liu, X., 2019. Quantifying the cooling-effects of urban and peri-urban wetlands using remote sensing data: case study of cities of Northeast China. Landsc. Urban Plann. 182, 92–100. https://doi.org/10.1016/j.landurbplan.2018.10.015.

Yang, S., Fang, X., Li, J., An, Z., Chen, S., Hitoshi, F., 2001. Transformation functions of soil color and climate. Sci. China Earth Sci. 44, 218–226. https://doi.org/10.1007/BF02911990.

Yonekura, Y., Ohta, S., Kiyono, Y., Aksa, D., Morisada, K., Tanaka, N., Kanzaki, M., 2010. Changes in soil carbon stock after deforestation and subsequent establishment of “Imperata” grassland in the Asian humid tropics. Plant Soil 329, 495–507. https://doi.org/10.1007/s11104-009-0175-y.

Yu, J., Wang, Y., Li, Y., Dong, H., Zhou, D., Han, G., Wu, H., Wang, G., Mao, P., Gao, Y., 2012. Soil organic carbon storage changes in coastal wetlands of the modern Yellow River Delta from 2000 to 2009. Biogeosciences 9, 2325–2331. https://doi.org/10.5194/bg-9-2325-2012.